Conflict of interest statement

The authors declare that there are no conflicts of interest.

Acknowledgments

This study was supported by the Grants-in-Aid for Scientific Research from the Ministry of Education, Culture, Sports, Science and Technology of Japan (nos. 21500352, 20023026, 21390271, 20023027, 18023033, 17300114); by the Grants-in-Aid for Comprehensive Research on Dementia from the Ministry of Health, Labour, and Welfare, Japan; and in part by the Alzheimer's Association (IIRG-09-132098).

References

Billings LM, Oddo S, Green KN, McGaugh JL, LaFerla FM. Intraneuronal Aβ causes the onset of early Alzheimer's disease-related cognitive deficits in transgenic mice. Neuron 2005;45:675–88.

Björkhem I. Crossing the barrier: oxysterols as cholesterol transporters and metabolic modulators in the brain. J Intern Med 2006;260:493–508.

Bodovitz S, Klein WL. Cholesterol modulates α-secretase cleavage of amyloid precursor protein. J Biol Chem 1996;271:4436–40.

D'Andrea MR, Nagele RG, Wang HY, Peterson PA, Lee DH. Evidence that neurones accumulating amyloid can undergo lysis to form amyloid plaques in Alzheimer's disease. Histopathology 2001;38:120–34.

Decker H, Lo KY, Unger SM, Ferreira ST, Silverman MA. Amyloid-β peptide oligomers disrupt axonal transport through an NMDA receptor-dependent mechanism that is mediated by glycogen synthase kinase 3β in primary cultured hippocampal neurons. J Neurosci 2010;30:9166–71.

De Felice FG, Wu D, Lambert MP, Fernandez SJ, Velasco PT, Lacor PN, et al. Alzheimer's disease-type neuronal tau hyperphosphorylation induced by Aβ oligomers. Neurobiol Aging 2008;29:1334–47.

Endoh R, Ogawara M, Iwatsubo T, Nakano I, Mori H. Lack of the carboxyl terminal sequence of tau in ghost tangles of Alzheimer's disease. Brain Res 1993;601:164–72.

Fernández-Vizarra P, Fernández AP, Castro-Blanco S, Serrano J, Bentura ML, Martínez-Murillo R, et al. Intra- and extracellular Aβ and PHF in clinically evaluated cases of Alzheimer's disease. Histol Histopathol 2004;19:823–44.

Fitz NF, Cronican A, Pham T, Fogg A, Fauq AH, Chapman R, et al. Liver X receptor agonist treatment ameliorates amyloid pathology and memory deficits caused by high-fat diet in APP23 mice. J Neurosci 2010;30:6862–72.

Friedrich RP, Tepper K, Rönicke R, Soom M, Westermann M, Reymann K, et al. Mechanism of amyloid plaque formation suggests an intracellular basis of Aβ pathogenicity. Proc Natl Acad Sci U S A 2010;107:1942–7.

Frears ER, Stephens DJ, Walters CE, Davies H, Austen BM. The role of cholesterol in the biosynthesis of β-amyloid. Neuroreport 1999;10:1699–705.

Gouras GK, Tsai J, Naslund J, Vincent B, Edgar M, Checler F, et al. Intraneuronal Aβ42 accumulation in human brain. Am J Pathol 2000;156:15–20.

Gouras GK, Tampellini D, Takahashi RH, Capetillo-Zarate E. Intraneuronal β-amyloid accumulation and synapse pathology in Alzheimer's disease. Acta Neuropathol 2010;119:523–41.

Greenberg SG, Davies P, Schein JD, Binder LI. Hydrofluoric acid-treated τ_{PHF} proteins display the same biochemical properties as normal τ. J Biol Chem 1992;267:564–9.

Grimm MOW, Grimm HS, Pätzold AJ, Zinser EG, Halonen R, Duering M, et al. Regulation of cholesterol and sphingomyelin metabolism by amyloid-β and presenilin. Nature Cell Biol 2005;7:1118–23.

Grimm MOW, Grimm HS, Tomic I, Beyreuther K, Hartmann T, Bergmann C. Independent inhibition of Alzheimer disease β- and γ-secretase cleavage by lowered cholesterol levels. J Biol Chem 2008;283:11302–11.

Gyure KA, Durham R, Stewart WF, Smialek JE, Troncoso JC. Intraneuronal Aβ-amyloid precedes development of amyloid plaques in Down syndrome. Arch Pathol Lab Med 2001;125:489–92.

Hsiao K, Chapman P, Nilsen S, Eckman C, Harigaya Y, Younkin S, et al. Correlative memory deficits, Aβ elevation, and amyloid plaques in transgenic mice. Science 1996;274:99-102.

Hu X, Crick SL, Bu G, Frieden C, Pappu RV, Lee JM. Amyloid seeds formed by cellular uptake, concentration, and aggregation of the amyloid-β peptide. Proc Natl Acad Sci U S A 2009;106:20324–9.

Ishibashi K, Tomiyama T, Nishitsuji K, Hara M, Mori H. Absence of synaptophysin near cortical neurons containing oligomer Aβ in Alzheimer's disease brain. J Neurosci Res 2006;84:632–6.

Ito K, Ishibashi K, Tomiyama T, Umeda T, Yamamoto K, Kitajima E, et al. Oligomeric amyloid β-protein as a therapeutic target in Alzheimer's disease: its significance based on its distinct localization and the occurrence of a familial variant form. Curr Alzheimer Res 2009;6:132–6.

Klein WL, Krafft GA, Finch CE. Targeting small Aβ oligomers: the solution to an Alzheimer's disease conundrum? Trends Neurosci 2001;24:219–24.

Knobloch M, Konietzko U, Krebs DC, Nitsch RM. Intracellular Abeta and cognitive deficits precede beta-amyloid deposition in transgenic arcAbeta mice. Neurobiol Aging 2007;28:1297–306.

Kurata T, Miyazaki K, Kozuki M, Panin VL, Morimoto N, Ohta Y, et al. Atorvastatin and pitavastatin improve cognitive function and reduce senile plaque and phosphorylated tau in aged APP mice. Brain Res 2011;1371:161–70.

LaFerla FM, Green KN, Oddo S. Intracellular amyloid-β in Alzheimer's disease. Nat Rev Neurosci 2007;8:499–509.

Lambert MP, Velasco PT, Chang L, Viola KL, Fernandez S, Lacor PN, et al. Monoclonal antibodies that target pathological assemblies of Aβ. J Neurochem 2007;100:23–35.

Lesné S, Koh MT, Kotilinek L, Kayed R, Glabe CG, Yang A, et al. A specific amyloid-β protein assembly in the brain impairs memory. Nature 2006;440:352–7.

Lippa CF, Ozawa K, Mann DM, Ishii K, Smith TW, Arawaka S, et al. Deposition of β-amyloid subtypes 40 and 42 differentiates dementia with Lewy bodies from Alzheimer disease. Arch Neurol 1999;56:1111–8.

Mori C, Spooner ET, Wisniewsk KE, Wisniewski TM, Yamaguch H, Saido TC, et al. Intraneuronal Aβ42 accumulation in Down syndrome brain. Amyloid 2002;9:88-102.

Nishitsuji K, Tomiyama T, Ishibashi K, Ito K, Teraoka R, Lambert MP, et al. The E693Δ mutation in amyloid precursor protein increases intracellular accumulation of amyloid β oligomers and causes endoplasmic reticulum stress-induced apoptosis in cultured cells. Am J Pathol 2009;174:957–69.

Oakley H, Cole SL, Logan S, Maus E, Shao P, Craft J, et al. Intraneuronal beta-amyloid aggregates, neurodegeneration, and neuron loss in transgenic mice with five familial Alzheimer's disease mutations: potential factors in amyloid plaque formation. J Neurosci 2006;26:10129–40.

Oddo S, Caccamo A, Shepherd JD, Murphy MP, Golde TE, Kayed R, et al. Triple-transgenic model of Alzheimer's disease with plaques and tangles: intracellular Aβ and synaptic dysfunction. Neuron 2003;39:409–21.

Oddo S, Caccamo A, Smith IF, Green KN, LaFerla FM. A dynamic relationship between intracellular and extracellular pools of Aβ. Am J Pathol 2006;168:184–94.

Petanceska SS, DeRosa S, Olm V, Diaz N, Sharma A, Thomas-Bryant T, et al. Statin therapy for Alzheimer's disease: will it work? J Mol Neurosci 2002;19:155–61.

Refolo LM, Malester B, LaFrancois J, Bryant-Thomas T, Wang R, Tint GS, et al. Hypercholesterolemia accelerates the Alzheimer's amyloid pathology in a transgenic mouse model. Neurobiol Dis 2000;7:321–31.

Schreurs BG. The effects of cholesterol on learning and memory. Neurosci Biobehav Rev 2010;34:1366–79.

Selkoe DJ. Alzheimer's disease is a synaptic failure. Science 2002;298:789–91.

Shie FS, Jin LW, Cook DG, Leverenz JB, LeBoeuf RC. Diet-induced hypercholesterolemia enhances brain Aβ accumulation in transgenic mice. Neuroreport 2002;13:455–9.

Simons M, Keller P, De Strooper B, Beyreuther K, Dotti CG, Simons K. Cholesterol depletion inhibits the generation of β-amyloid in hippocampal neurons. Proc Natl Acad Sci U S A 1998;95:6460–4.

Solomon A, Kivipelto M. Cholesterol-modifying strategies for Alzheimer's disease. Expert Rev Neurother 2009;9:695–709.

Stefani M, Liguri G. Cholesterol in Alzheimer's disease: unresolved questions. Curr Alzheimer Res 2009;6:15–29.

Takahashi RH, Milner TA, Li F, Nam EE, Edgar MA, Yamaguchi H, et al. Intraneuronal Alzheimer Aβ42 accumulates in multivesicular bodies and is associated with synaptic pathology. Am J Pathol 2002;161:1869–79.

Tampellini D, Capetillo-Zarate E, Dumont M, Huang Z, Yu F, Lin MT, et al. Effects of synaptic modulation on β-amyloid, synaptophysin, and memory performance in Alzheimer's disease transgenic mice. J Neurosci 2010;30:14299–304.

Tomiyama T, Nagata T, Shimada H, Teraoka R, Fukushima A, Kanemitsu H, et al. A new amyloid β variant favoring oligomerization in Alzheimer's-type dementia. Ann Neurol 2008;63:377–87.

Tomiyama T, Matsuyama S, Iso H, Umeda T, Takuma H, Ohnishi K, et al. A mouse model of amyloid β oligomers: their contribution to synaptic alteration, abnormal tau phosphorylation, glial activation, and neuronal loss in vivo. J Neurosci 2010;30:4845–56.

Ullrich C, Pirchl M, Humpel C. Hypercholesterolemia in rats impairs the cholinergic system and leads to memory deficits. Mol Cell Neurosci 2010;45:408–17.

Umeda T, Mori H, Zheng H, Tomiyama T. Regulation of cholesterol efflux by amyloid β secretion. J Neurosci Res 2010;88:1985–94.

Umeda T, Tomiyama T, Sakama N, Tanaka S, Lambert MP, Klein WL, et al. Intraneuronal amyloid β oligomers cause cell death via endoplasmic reticulum stress, endosomal/lysosomal leakage, and mitochondrial dysfunction in vivo. J Neurosci Res 2011;89:1031–42.

Wegenast-Braun BM, Fulgencio Maisch A, Eicke D, Radde R, Herzig MC, Staufenbiel M, et al. Independent effects of intra- and extracellular Aβ on learning-related gene expression. Am J Pathol 2009;175:271–82.

Wirths O, Multhaup G, Bayer TA. A modified β-amyloid hypothesis: intraneuronal accumulation of the β-amyloid peptide — the first step of a fatal cascade. J Neurochem 2004;91:513–20.

Xiong H, Callaghan D, Jones A, Walker DG, Lue LF, Beach TG, et al. Cholesterol retention in Alzheimer's brain is responsible for high β- and γ-secretase activities and Aβ production. Neurobiol Dis 2008;29:422–37.

Neurochemistry International 61 (2012) 347–355

Contents lists available at SciVerse ScienceDirect

Neurochemistry International

journal homepage: www.elsevier.com/locate/nci

Proteomic analysis of the brain tissues from a transgenic mouse model of amyloid β oligomers

Masaoki Takano [a], Kouji Maekura [a], Mieko Otani [a], Keiji Sano [a], Tooru Nakamura-Hirota [b], Shogo Tokuyama [c], Kyong Son Min [d], Takami Tomiyama [e], Hiroshi Mori [e,f], Shogo Matsuyama [b,*]

[a] Department of Life Sciences Pharmacy, School of Pharmaceutical Sciences, Kobe Gakuin University, 1-1-3 Minatojima, Chuo-ku, Kobe 650-8586, Japan
[b] Faculty of Pharmaceutical Sciences, Himeji Dokkyo University, 7-2-1 Kamiohno, Himeji 670-8524, Japan
[c] Department of Clinical Pharmacy, School of Pharmaceutical Sciences, Kobe Gakuin University, 1-1-3 Minatojima, Chuo-ku, Kobe 650-8586, Japan
[d] Laboratory of Toxicology, Faculty of Pharmacy, Osaka Ohtani University, 3-11-1 Nishikigorikita, Tondabayashi, Osaka 584-8540, Japan
[e] Department of Neuroscience and Neurology, Osaka City University Graduate School of Medicine, Osaka 545-8585, Japan
[f] Core Research for Evolutional Science and Technology, Japan Science and Technology Agency, Japan

ARTICLE INFO

Article history:
Received 3 October 2011
Received in revised form 11 May 2012
Accepted 14 May 2012
Available online 23 May 2012

Keywords:
Proteome
Amyloid β oligomers
Alzheimer's disease
Hippocampus
Cortex
Phosphoproteome

ABSTRACT

Amyloid β (Aβ) oligomers are presumed to be one of the causes of Alzheimer's disease (AD). Previously, we identified the E693Δ mutation in amyloid precursor protein (APP) in patients with AD who displayed almost no signals of amyloid plaques in amyloid imaging. We generated APP-transgenic mice expressing the E693Δ mutation and found that they possessed abundant Aβ oligomers from 8 months of age but no amyloid plaques even at 24 months of age, indicating that these mice are a good model to study pathological effects of Aβ oligomers. To elucidate whether Aβ oligomers affect proteome levels in the brain, we examined the proteins and phosphoproteins for which levels were altered in 12-month-old $APP_{E693\Delta}$-transgenic mice compared with age-matched non-transgenic littermates. By two-dimensional gel electrophoresis (2DE) followed by staining with SYPRO Ruby and Pro-Q Diamond and subsequent mass spectrometry techniques, we identified 17 proteins and 3 phosphoproteins to be significantly changed in the hippocampus and cerebral cortex of $APP_{E693\Delta}$-transgenic mice. Coactosin like-protein, SH3 domain-bind glutamic acid-rich-like protein 3 and astrocytic phosphoprotein PEA-15 isoform 2 were decreased to levels less than 0.6 times those of non-transgenic littermates, whereas dynamin, profilin-2, vacuolar adenosine triphosphatase and creatine kinase B were increased to levels more than 1.5 times those of non-transgenic littermates. Furthermore, 2DE Western Blotting validated the changed levels of dynamin, dihydropyrimidinase-related protein 2 (Dpysl2), and coactosin in $APP_{E693\Delta}$-transgenic mice. Glyoxalase and isocitrate dehydrogenase were increased to levels more than 1.5 times those of non-transgenic littermates. The identified proteins could be classified into several groups that are involved in regulation of different cellular functions, such as cytoskeletal and their interacting proteins, energy metabolism, synaptic component, and vesicle transport and recycling. These findings indicate that Aβ oligomers altered the levels of some proteins and phosphoproteins in the hippocampus and cerebral cortex, which could illuminate novel therapeutic avenues for the treatment of AD.

1. Introduction

Alzheimer's disease (AD) is the most frequent neurodegenerative disorder and the most common cause of dementia in the elderly (Lee et al., 2001). AD is neuropathologically characterized by abnormal accumulation of extracellular amyloid plaques and intracellular neurofibrillary tangles throughout cortical and limbic regions. There are numerous, complex pathological changes in AD brain that contribute to neural and synaptic degeneration, including mitochondrial dysfunction, oxidative damage, and inflammation (Akiyama et al., 2000; Glenner and Wong, 1984; Nunomura et al., 2001). Although the current amyloid cascade hypothesis (Hardy and Selkoe, 2002) and tau hypothesis (Lee et al., 2001) provide frameworks for studying AD pathogenesis, the detailed molecular mechanisms that translate amyloid or tau accumulation into neural damage and functional brain impairments are largely unknown. Recently, diverse lines of evidence suggest that amyloid-beta (Aβ) peptides play more important roles in AD pathogenesis (Klein et al., 2001; Li et al., 2009; Selkoe, 2002). Especially, soluble oligomers of Aβ could be a cause of synaptic and cognitive dysfunction in the early stage of AD.

We previously identified the E693Δ mutation in amyloid precursor protein (APP) in patients with AD who displayed almost

* Corresponding author.
E-mail address: shogo@himeji-du.ac.jp (S. Matsuyama).

0197-0186/$ - see front matter © 2012 Elsevier Ltd. All rights reserved.
http://dx.doi.org/10.1016/j.neuint.2012.05.018

no signals of amyloid plaques in amyloid imaging (Tomiyama et al., 2008). To address the relationship between Aβ oligomers and pathological features of AD, we generated APP transgenic mice expressing the E693Δ mutation, which enhanced Aβ oligomerization without fibrillization (Tomiyama et al., 2011). The $APP_{E693\Delta}$-transgenic mice displayed age-dependent accumulation of intraneuronal Aβ oligomers from 8 months and showed impairment of hippocampal synaptic plasticity and memory at 8 months, abnormal tau phosphorylation from 8 months, glial activation from 12–18 months, and neuronal loss at 24 months, but no amyloid plaques even at 24 months (Tomiyama et al., 2011). Thus, the $APP_{E693\Delta}$-transgenic mice might become a useful model to elucidate Aβ oligomer-dependent pathways in AD pathology.

The $APP_{E693\Delta}$-transgenic mouse model might provide a clue for elucidating AD pathology to detect proteomic alteration caused by Aβ oligomers in the brain. One of the most utilized approaches in proteomics to quantify and identify proteins is 2DE and mass spectrometry (MS)(Gorg et al., 2000). This proteomic approach as revealed differential levels of proteins expressed in the brains of AD patients (Sultana et al., 2007), mutant APP transgenic mice (Shin et al., 2004), and mutant tau transgenic mice (Takano et al., 2009). Using the 2DE and MS approach, we identified 17 proteins and 3 phosphoproteins for which levels were altered in the hippocampus and cerebral cortex of 12-month-old $APP_{E693\Delta}$-transgenic mice compared with age-matched non-transgenic littermates. These proteins might play pivotal roles in the early stage of AD.

2. Experimental procedures

2.1. Materials

Sodium dodecyl sulfate, urea, thiourea, CHAPS, dithiothreitol, iodoacetamide, bromo phenol blue, and RNase A and DNase I for SDS–PAGE or 2DE were all obtained from Wako Pure Chemical Industries (Osaka, Japan). Source information for all other assay reagents and materials are incorporated into their respective assay methods described below.

2.2. Animal subjects

Transgenic mice expressing human APP_{695} with the $APP_{E693\Delta}$ mutation under the mouse prion promoter (Tomiyama et al., 2011) were used. Heterozygous human $APP_{E693\Delta}$-transgenic mice and age-matched non-transgenic littermates were sacrificed at 12 months of age, and their hippocampi and cortices were isolated on an ice-cold plate. Animal care and handling were performed strictly in accordance with the Guidelines for Animal Experimentation at Kobe Gakuin University and Himeji Dokkyo University. Every effort was made to minimize the number of animals used and their suffering.

2.3. Sample preparation

The isolated hippocampus and cortex were transferred to a 1.5-ml tube, centrifuged (15,000g, 5 min at 4 °C), resuspended in 100 μl of lysis buffer (7 M urea, 2 M thiourea, 5% CHAPS, 2% IPG buffer [GE Healthcare UK Ltd., England], 50 mM 2-mercaptoethanol, 2.5 μg/ml DNase I, 2.5 μg/ml RNase A), and disrupted by sonication for 30 s. Lysate was again centrifuged (15,000g, 30 min) to remove cellular debris, and the supernatant was recovered for use in 2DE.

2.4. Two-dimensional electrophoresis

2DE was carried out by the method as previously described (Otani et al., 2011) with minor modifications. Approximately 500 μg of protein was applied to ImmobilineDryStrip pH 3–10 NL (7 cm) gels (GE Healthcare UK Ltd., England) and separated at 50 V for 6 h, at 100 V for 6 h, and at 2000 V for 6 h. The immobilised pH gradient (IPG) strips were equilibrated for 15 min in 50 mM Tris/HCl (pH8.8), 6 M urea, 30% (v/v) glycerol, 1% SDS, and 1% (v/v) DTT, and then for 15 min in the same buffer with 2.5% (w/v) iodoacetamide instead of DTT. After equilibration, the IPG strips were set onto a 12.5% acrylamide gel and SDS–polyacrylamide gel electrophoresis was performed at 5 mA/gel for 7 h.

2.5. SYPRO Ruby staining

Proteins on SDS–polyacrylamide gels were detected using the SYPRO Ruby Protein Gel Stain (Molecular Probes). Gels after 2DE were fixed in a solution containing 10% acetic acid/50% methanol for 30 min, then 7% acetic acid/10% methanol for 30 min. After fixing, the gels were incubated in the undiluted stock solution of SYPRO Ruby for 90 min, and destained with 7% acetic acid/10% methanol for 30 min. After rinsing with H_2O for 10 min, digital images were acquired using a Fluorophorestar 3000 image capture system (Anatech, Japan) with 470 nm excitation and 618 nm emission for SYPRO Ruby detection.

2.6. Pro-Q Diamond staining

Phosphoproteins on SDS–polyacrylamide gels were detected using Pro-Q Diamond Phosphoprotein Stain (Molecular Probes). Gels after 2DE were fixed in a solution containing 10% acetic acid/50% methanol for 30 min two times, and then the gels were washed with MilliQ H_2O for 10 min twice. The gels were then incubated in an undiluted stock solution of Pro-Q Diamond for 90 min, and destained with three successive washes (30 min per wash) in 50 mM sodium acetate (pH 4.0), 20% (v/v) acetonitrile. Digital images were acquired using the Fluorophorestar 3000 image capture system with 520 nm excitation and 575 nm emission for Pro-Q Diamond detection.

2.7. Image analysis

Following image acquisition, 2D gel imaging and analysis software Prodigy SameSpots (Nonlinear Dynamics, UK) version 1.0 was used for gel-to-gel matching and identifying differences between non-transgenic and mutant APP transgenic mouse samples. Each of five sets of samples was represented by two independent gels biological replicates of 2DE gels. The gel images were normalized in the Prodigy SameSpots software to even out differences in staining intensities among gels. ANOVA was performed with 95% significance level to determine which proteins were differentially expressed between the non-transgenic and mutant APP transgenic mice. A minimum of 1.3-fold change was considered to identify the increased proteins and 0.7-fold change for decreased proteins.

2.8. In-gel digestion and peptide extraction

In-gel digestion was performed in accordance with the method of (Yokoyama et al., 2004). Protein spots in the gels stained with SYPRO Ruby or Pro-Q Diamond were cut out and subjected to trypsin digestion with porcine trypsin (Promega, Madison, WI, USA). Briefly, gel pieces were washed, dehydrated, and diluted in 200 μl of 25 mM ammonium hydrogen carbonate with 5% ACN

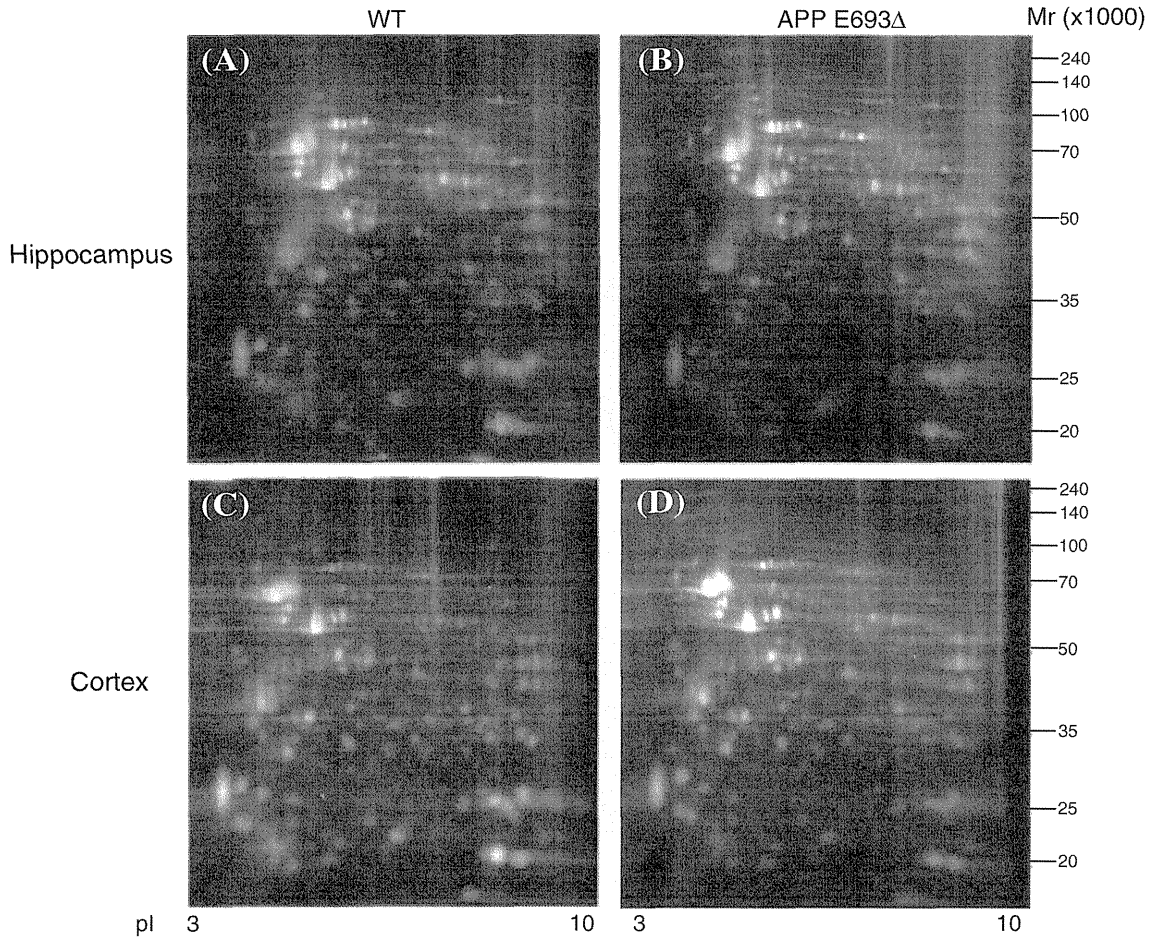

Fig. 1. SYPRO Ruby-stained 2DE gels (pH range 3–10) for the hippocampus and cerebral cortex from non-transgenic and $APP_{E693\Delta}$-transgenic mice. To each gel, 500 μg of protein was loaded for detection of protein expression. (A) Hippocampus of wild-type (or non-transgenic) littermates, (B) hippocampus of $APP_{E693\Delta}$-transgenic mice, (C) cortex of wild-type (or non-transgenic) littermates and (D) cortex of $APP_{E693\Delta}$-transgenic mice. Protein molecular mass standards (*y*-axis) and pHs (*x*-axis) are shown.

(v/v). Trypsin (5 μl, 10 ng/μl) was added and the digestion was incubated for 10 h at 37 °C. After separation of supernatant, gel pieces were washed again and then extracted with 50/50 ACN/0.3% (v/v) trifluoroacetic acid for 10 min by sonication. The supernatant was once again collected, mixed with the two fractions, and evaporated under vacuum. The extracted peptides were then diluted in 5 μl of 50/50 ACN/0.3% (v/v) trifluoroacetic acid.

2.9. Mass spectrometry analysis and protein identification

Mass spectra were recorded in positive reflection mode using a MALDI-TOF MS/MS analyzer (ABI PLUS 4800, Applied Biosystems), equipped with a delayed ion technology. The samples were dissolved in 5 μl of 50/50 ACN/0.3% (v/v) trifluoroacetic acid. For the matrix, α-cyano-4-hydroxycinnamic acid (1 μg/μl: Wako Junyaku, Osaka, Japan) dissolved in the same mixture was used. Analyte and matrix were spotted consecutively in a 1:1 ratio on a stainless steel target and dried under ambient conditions. All spectra acquired by MALDI-TOF MS were externally calibrated with peptide calibration standard II (Bruker Daltonics, Germany). An MS condition of 2500 shots per spectrum was used. Automatic monoisotopic precursor selection for MS/MS was done using an interpretation method based on the 12 most intense peaks per spot with an MS/MS mode condition of 4000 laser shots per spectrum. Minimum peak width was one fraction and mass tolerance was 80 ppm. Adduct tolerance was $(m/z) \pm 0.003$. MS/MS was performed with a gas pressure of 1×10^{-6} bar in the collision cell. Ambient air was used as collision gas. Data analyses were performed using Data Explorer version 4.9 (Applied Biosystems) software, and proteins were identified through the search engine Mascot (www.matrixscience.com; Matrix Science, Boston, MA) (peptide mass tolerance: 60 ppm; MS/MS tolerance: 0.3 Da; maximum missed cleavages: 1) using the protein database NCBInr. Proteins identified by MALDI-TOF MS with a score of 79 or higher were considered significant ($p < 0.05$). Single peptides identified by MALDI–TOF/TOF MS/MS with individual ions scores greater than 47 indicate identity or extensive homology ($p < 0.05$).

2.10. 2DE Western Blotting

Approximately 100 μg of protein from mouse hippocampus was applied to ImmobilineDryStrip pH 3–10 NL (7 cm) gel in first dimension, and then the IPG strips were set onto a 10.0% acrylamide gel and SDS–polyacrylamide gel electrophoresis was performed at 5 mA/gel for 7 h in second dimension. The gels were transferred onto PVDF membranes (Pall Corporation, Pensacola, FL, USA), in a trans-blot electrophoresis transfer cell (Nihon Eido, Tokyo, Japan). Western Blotting were performed by using monoclonal antibodies against dynamin (diluted 1:1000, Cell Signaling, USA), polyclonal antibodies Dpysl2, coactosin and voltage-dependent anion-selective channel protein 1 (VDAC) (diluted 1:1000, Cell Signaling, USA). Peroxidase-conjugated antibody (diluted 1:5000, Abcam, USA) was used as secondary antibody. The reaction was detected by chemiluminescence with ECL reagents (Pierce Biotechnology, USA). A semi quantitative analysis based on optical density was

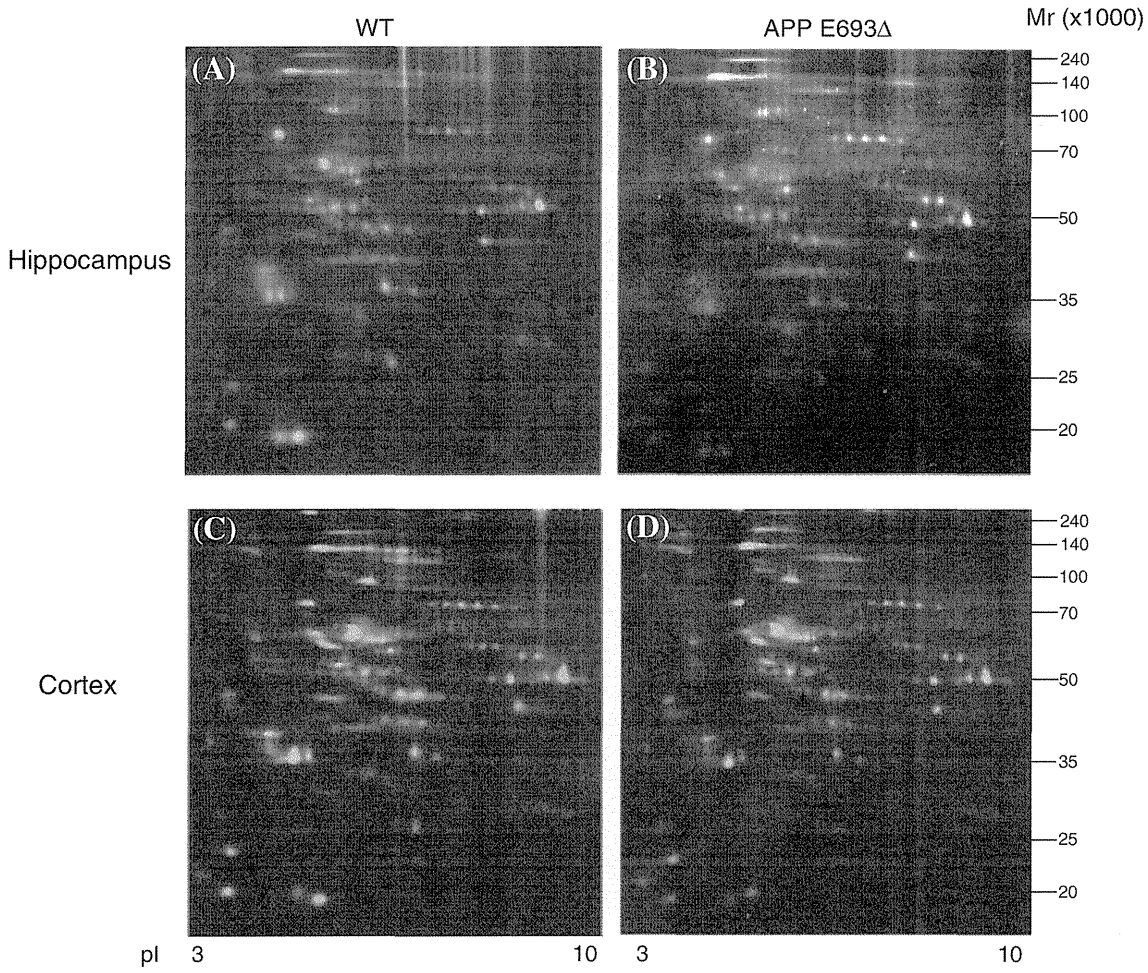

Fig. 2. Pro-Q Diamond-stained 2DE gels for the hippocampus and cerebral cortex from non-transgenic and $APP_{E693\Delta}$-transgenic mice. To each gel, 500 μg of protein was loaded for detection of protein expression. (A) Hippocampus of wild-type (or non-transgenic) littermates, (B) hippocampus of $APP_{E693\Delta}$-transgenic mice, (C) cortex of wild-type (or non-transgenic) littermates and (D) cortex of $APP_{E693\Delta}$-transgenic mice. Protein molecular mass standards (*y*-axis) and pHs (*x*-axis) are shown.

performed by ImageJ software (available at http://www.rsbweb.nih.gov/ij).

3. Results

The levels of proteins and phosphoproteins in the hippocampus and cerebral cortex of $APP_{E693\Delta}$-transgenic mice were compared to those of non-transgenic littermates. The altered levels of proteins and phosphoproteins were quantified and identified from 2DE gels using Prodigy SameSpots software for MALDI–MS/MS. We showed representative 2DE gels stained with SYPRO Ruby and Pro-Q Diamond for the hippocampus and cerebral cortex of non-transgenic mice and $APP_{E693\Delta}$-transgenic mice (Figs. 1 and 2) and the raw data for the reproducibility of 2DE gels (Supplementary Fig. 1A–D). There were approximately 350 spots in each SYPRO Ruby-stained 2DE gel from hippocampus and cortex of WT and $APP_{E693\Delta}$-transgenic mice (Fig. 1A-D), and approximately 270 spots in each ProQ Diamond-stained 2DE gel from hippocampus and cortex of WT and $APP_{E693\Delta}$-transgenic mice (Fig. 2A-D). The indicated spots of 2DE gels showed altered levels of proteins (Fig. 3), for which spots were excised according to the Prodigy program. Comparing the intensity of protein spots from the hippocampus and cerebral cortex of $APP_{E693\Delta}$-transgenic mice to those of non-transgenic mice, the levels of 70 protein spots (ANOVA < 0.05, fold > 1.3 or <0.7) and 17 phosphoprotein spots (ANOVA < 0.05, fold > 1.3 or <0.7) were altered. Finally, the total 22 polypeptides were identified, including 15 polypeptides in SYPRO Ruby-stained gel from hippocampus (Table 1), 7 polypeptides in SYPRO Ruby-stained gel from cortex (Table 2), and 3 polypeptides in ProQ Diamond-stained gel from hippocampus (Table 3). We also showed the raw data of spot intensities about the reproducibility of their bioinformatic analysis (Supplementary Fig. 2A–C).

3.1. Identification of altered proteins in $APP_{E693\Delta}$-transgenic mice hippocampus

Protein levels were significantly decreased for coactosin-like protein, SH3 domain-bind glutamic acid-rich-like protein3, astrocytic phosphoprotein PEA-15 isoform 2, dual specificity protein phosphatase 3, and phosphatidylethanolamine-binding protein, and increased for dynamin, profilin-2, vacuolar adenosine triphosphatase subunit B, transketolase, Dpysl2, Atp5b protein and fascin in the hippocampus (Table 1). To benchmark the proteomic analysis, we chose VDAC and MDH 2 as common, non-regulated proteins. Protein levels of VDAC and MDH 2 were not changed in the hippocampus of $APP_{E693\Delta}$-transgenic mice, compared to non-transgenic mice (Table 1).

3.2. Identification of altered proteins in $APP_{E693\Delta}$-transgenic mice cortex

Protein levels were significantly decreased for profilin-2, LMW phosphotyrosine protein phosphatase isoform 2, coactosin-like

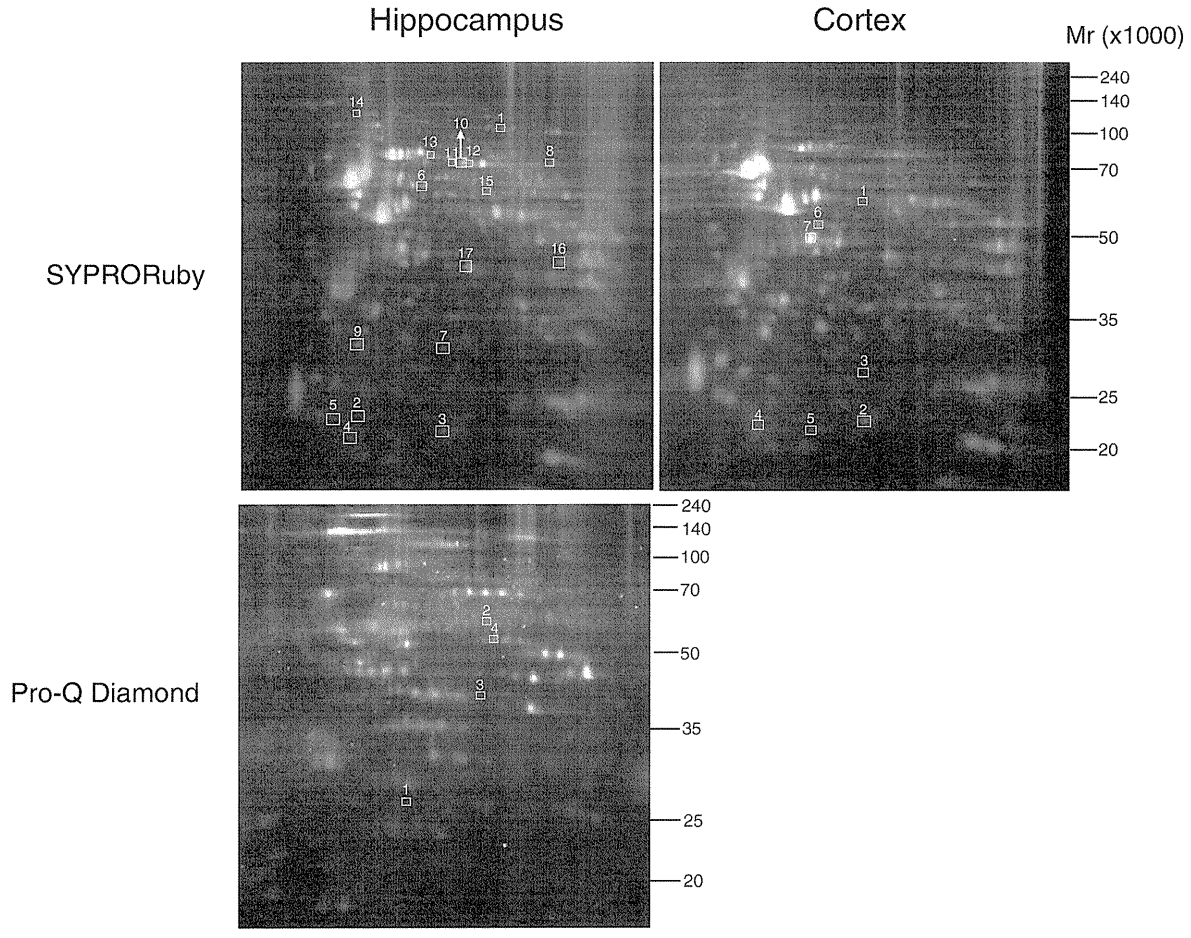

Fig. 3. A match set of the proteins differently expressed in $APPE_{693\Delta}$-transgenic mice brains by Prodigy. In SYPRO Ruby-stained gels, 15 spots were identified in the hippocampus and 7 spots were in the cortex. Four spots were identified as phosphoproteins in the hippocampus in Pro-Q Diamond-stained gels. The numbers indicated, correspond to the spot numbers in Tables 1–3.

protein and fatty acid-binding protein, and increased for creatine kinase B type, isocitrate dehydrogenase and guanine nucleotide binding protein in the cortex (Table 2).

3.3. *Identification of altered phosphoproteins in $APP_{E693\Delta}$-transgenic mice hippocampus*

The significantly decreased phosphoprotein was vacuolar adenosine triphosphatase, and the significantly increased phosphoproteins were glyoxalase and isocitrate dehydrogenase in the hippocampus (Table 3).

3.4. *Validation of dynamin, Dpysl2, coactosin and VDAC levels by 2DE Western Blotting*

We performed 2DE Western Blotting as a validation experiment for dynamin, Dpysl2 and coactosin as the altered proteins, and VDAC as the unchanged protein (as control). Relative abundance of each band measured by the optical density was evaluated by ImageJ software. Relative abundance of dynamin was 100.0 ± 18.3 in non-transgenic mice and 177.6 ± 15.6 in $APP_{E693\Delta}$-transgenic mice ($p < 0.05$). Relative abundance of Dpysl2 was 100.0 ± 47.4 in non-transgenic mice and 158.2 ± 24.6 in $APP_{E693\Delta}$-transgenic mice (not significant). Relative abundance of coactosin was 100.0 ± 24.5 in non-transgenic mice and 27.9 ± 16.9 in $APP_{E693\Delta}$-transgenic mice ($p < 0.05$). Relative abundance of VDAC was 100.0 ± 10.9 in non-transgenic mice and 129.3 ± 6.6 in $APP_{E693\Delta}$-transgenic mice (not significant). Thus, the increased levels of dynamin and Dpysl2, the decreased levels of coactosin, and the unchanged level of VDAC as control in $APP_{E693\Delta}$-transgenic mice hippocampus were validated by 2DE Western Blotting.

4. Discussion

In this study, using 2DE coupled with MS, we identified 17 proteins and 3 phosphoproteins that showed differential levels in $APP_{E693\Delta}$-transgenic mouse hippocampus and cortex. Furthermore, some of these proteins were validated by 2DE Western Blotting (Fig. 4). These proteins and phosphoproteins were classified into several groups on a functional basis, by using MOTIF (http://www.genome.jp/tools/motif/) database, as shown in Tables 4 and 5. Previous proteomics studies showed altered levels of metabolism proteins, synaptic process, pH regulation, and antioxidant functional proteins in brains of 3xTgAD and Tg2576 mice and the hippocampus of AD patients (Martin et al., 2008; Shin et al., 2004; Sultana et al., 2007). However, as there were many amyloid plaques in their brains, it was difficult to distinguish which levels of proteins and phosphoproteins were altered by soluble Aβ oligomers or by insoluble Aβ fibrils. In contrast, the $APP_{E693\Delta}$-transgenic mice used in the present study were shown to exhibit only Aβ oligomer accumulation even at 24 months of age. Therefore, the proteomic alterations observed in $APP_{E693\Delta}$-transgenic mice could be attributable to Aβ oligomers, although we cannot exclude the

Table 1
Differentially expressed proteins in $APP_{E693\Delta}$-transgenic mouse hippocampus when compared to non-transgenic littermates ($n = 5$).

Spot No.	GI acc. No.	Identified protein	Theoretical MW/pI	Practical MW (kDa)/pI	Score	SC	Number of peptides	ANOVA	Fold increase/decrease
1	487851	Dynamin	85329/5.97	85/7.1	250	5	3	0.004	2.3
2	159163110	Coactosin-like protein	16623/5.13	15/5.2	153	25	4	2.45E-04	0.6
3	9506971	Profilin-2	15364/6.55	14/5.9	130	20	4	0.014	1.7
4	18017602	SH3 domain-bind glutamic acid-rich-like protein3	10527/5.02	13/5.1	140	16	2	0.019	0.6
5	2142847	Astrocytic phosphoprotein PEA-15 isoform 2	15102/4.94	14/5.1	202	13	3	0.035	0.6
6	1184661	Vacuolar adenosine triphosphatase subunit B	56948/5.57	55/5.7	311	11	5	0.029	1.5
7	21312314	Dual specificity protein phosphatase 3	20687/6.07	20/6.0	236	17	2	0.002	0.7
8	6678359	Transketolasc	68272/7.23	65/8.6	126	8	3	0.007	1.4
9	84794552	Phosphatidylethanolamine-binding protein	20991/5.19	20/5.2	105	25	3	0.021	0.7
10	40254595	Dihydropyrimidinase-related protein 2	62638/5.95	70/6.3	382	10	5	0.017	1.4
11	40254595	Dihydropyrimidinase-related protein 2	62638/5.95	70/6.1	434	11	5	0.017	1.4
12	40254595	Dihydropyrimidinase-related protein 2	62638/5.95	70/6.4	540	16	6	0.009	1.3
13	40254595	Dihydropyrimidinase-related protein 2	62638/5.95	70/6.0	291	11	5	0.049	1.3
14	23272966	Atp5b protein	56632/5.24	12/5.2	496	14	6	0.032	1.3
15	113680348	Fascin	55215/6.44	50/6.8	129	10	3	0.017	1.3
16	6755963	Voltage-dependent anion-selective channel protein 1	30851/8.62	33/4.0	150	13	2	NS	1.0
17	387129	Malate dehydrogenase 2	36625/6.16	35/6.0	101	12	3	NS	1.0

The proteins of mouse hippocampus were separated by 2DE and identified by MALDI-TOF MS/MS, following in-gel digestion with trypsin. The spots representing the identified proteins are indicated in Fig. 3 and are designated with their gene ID accession numbers (GI acc. No.) of Swiss Prot database. Score relates to the probability assignment, theoretical molecular weight, and pI, and sequence coverage (SC) values are given. Score and sequence coverage were calculated by MASCOT search engine (http://www.matrixscience.com). Data were analyzed by ANOVA. NS: not significantly differences.

Table 2
Differentially expressed proteins in $APP_{E693\Delta}$-transgenic mouse cortex when compared to non-transgenic littermates ($n = 5$).

Spot No.	GI acc. No.	Identified protein	Theoretical MW/pI	Practical MW (kDa)/pI	Score	SC	Number of peptides	ANOVA	Fold increase/decrease
1	10946574	Creatine kinase Btype	42971/5.4	65/8.0	112	8	3	0.029	1.6
2	9963901	Profilin-2	16056/6.55	15/5.5	136	19	4	0.001	0.7
3	31542070	LMW phosphotyrosine protein phosphatase	18636/6.3	18/6.0	100	17	5	0.031	0.7
4	19482160	Coactosin-like protein	16048/5.28	15/4.5	303	44	4	0.001	0.7
5	6753810	Fatty acid-binding protein	14810/6.11	13/6.0	114	32	3	0.003	0.7
6	18250284	Isocitrate dehydrogenase	40069/6.27	50/5.5	158	6	2	0.024	1.3
7	6680045	Guanine nucleotide binding protein	38151/5.6	42/5.5	160	11	2	0.004	1,3

The proteins of mouse cortex were separated by 2DE and identified by MALDI-TOF MS/MS, following in-gel digestion with trypsin. The spots representing the identified proteins are indicated in Fig. 3 and are designated with their gene ID accession numbers (GI acc. No.) of Swiss Prot database. Score relates to the probability assignment, theoretical molecular weight, and pI, and sequence coverage (SC) values are given. Score and sequence coverage were calculated by MASCOT search engine (http://www.matrixscience.com).

possibility that the alterations were induced by the overexpression of human APP itself, which remains to be studied.

4.1. Cytoskeletal and their interacting proteins

Cytoskeletal proteins regulate several types of functions in neurons. Several proteins involved in cytoskeletal and their interacting proteins were affected in the mutant APP transgenic mice (Sultana et al., 2007). Actin is one of the major cytoskeletal proteins in neurons, and the dynamics of its assembly are involved in many aspects of cell motility, vesicle transport, and membrane turnover (Kuhn et al., 2000). In the present study, coactosin-like protein and profilin-2 were differentially expressed as actin-related proteins. The significantly decreased coactosin-like protein being belongs to the cofilin family protein (Minamide et al., 2000; Provost et al., 2001), which is an actin-binding protein and critically controls actin filament dynamics and reorganization by severing and depolymerizing actin filaments (Whiteman et al., 2009). On the

Table 3
Differentially expressed phosphoproteins in $APP_{E693\Delta}$-transgenic mouse hippocampus when compared to non-transgenic littermates ($n = 5$).

Spot No.	GI acc. No.	Identified protein	Theoretical MW/pI	Practical MW (kDa)/pI	Score	SC	Number of peptides	ANOVA	Fold increase/ decrease
1	19354350	Glyoxalase	20997/5.24	20/5.5	130	9	2	0.002	1.5
2	1184661	Vacuolar adenosine triphosphatase subunit B	56948/5.57	50/5.0	446	14	5	0.01	0.7
3	18250284	Isocitrate dehydrogenase	40069/6.27	30/5.0	206	6	2	0.036	1.5
4	1184661	Vacuolar adenosine triphosphatase subunit B	56948/5.57	50/5.0	289	11	4	0.006	0.71

The proteins of mouse hippocampus were separated by 2DE and identified by MALDI–TOF MS/MS, following in-gel digestion with trypsin. The spots representing the identified proteins are indicated in Fig. 3 and are designated with their gene ID accession numbers (GI acc. No.) of Swiss Prot database. Score relates to the probability assignment, theoretical molecular weight, and pI, and sequence coverage (SC) values are given. Score and sequence coverage were calculated by MASCOT search engine (http://www.matrixscience.com).

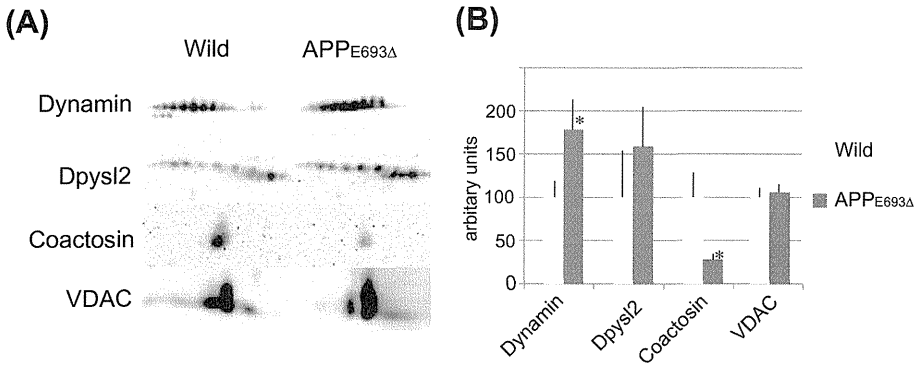

Fig. 4. Differentially expressed proteins validated by 2DE Western blotting for the hippocampus of non-transgenic and $APP_{E693\Delta}$-transgenic mice. (A) The levels of dynamin, Dpysl2, coactosin and VDAC in individual samples of each group were detected. (B) Graphical representation of the semi quantitative analysis. (mean ± S.E.M. of O.D. of bands). Data are presented as mean ± S.E.M. ANOVA; $^*P < 0.05$non-transgenic vs $APP_{E693\Delta}$-transgenic mice.

Table 4
Functions regulated by proteins that showed an altered expression in $APPE_{693\Delta}$-transgenic mouse hippocampus and cortex.

SyproRuby Function	Region	Identified protein	up/down
Cytoskeletal and their interacting proteins	hip., cor.	Coactosin-like protein	down
	hip.	Profilin-2	up
	hip.	Fascin	up
	cor.	Profilin-2	down
Metabolism	hip.	Transketolase	up
	hip.	Atp5b protein	up
	cor.	Creatine kinase Btype	up
	hip.	Isocitrate dehydrogenase	up
Synaptic component	hip.	Vacuolar adenosine triphosphatase subunit B	up
	hip.	Dual specificity protein phosphatase 3	down
	hip.	Phosphatidylethanolamine-binding protein	down
	hip.	Dihydropyrimidinase-related protein 2	up
	cor.	Fatty acid-binding protein	down
Vesicle Transport and Recycling	hip.	Dynamin	up
Other	hip.	SH3 domain-bind glutamic acid-rich-like protein3	down
	hip.	Astrocytic phosphoprotein PEA-15 isoform 2	down
	cor.	LMW phosphotyrosine protein phosphatase isoform 2	down

The analysis of proteins function was by using MOTIF (http://www.genome.jp/tools/motif/).

contrary, profilin-2, a subtype of profilin, was significantly increased. Profilin binds to monomeric actin, thereby occupying an actin-actin contact site; in effect, profilin sequesters actin from the pool of polymerizable actin monomers (Birbach, 2008). Interestingly, actin itself is known to link with tau and Aβ. Tau induces changes in the organization and stability of neuronal actin filaments, which in turn contribute to Alzheimer's-like neurodegeneration in *Drosophila* and mouse model systems for AD (Fulga et al., 2007). Aβ also enhances the neurotoxicity induced by tau-mediated actin filament formation (Fulga et al., 2007). These observations join a growing body of evidence indicating that alterations in the actin cytoskeleton may underlie the neuropathology of

Table 5
Functions regulated by phosphoproteins that showed an altered expression in $APP_{E693\Delta}$-transgenic mouse hippocampus.

ProQ Diamond Function	Region	Identified protein	up/down
Metabolism	hip.	Glyoxalase	up
	hip.	Isocitrate dehydrogenase	up
Synaptic component	hip.	Vacuolar adenosine triphosphatase subunit B	down

The analysis of proteins function was by using MOTIF (http://www.genome.jp/tools/motif/).

Alzheimer's disease and related fronto-temporal dementias in humans.

4.2. Energy metabolism

Glucose metabolism is highly important as an energy source in the brain, as the function of glucose in the brain has been considered solely related to ATP production (Vanhanen et al., 2006). Energy metabolic enzymes affected AD and AD model mice in the pathological processes (Hoyer, 2004). Our results showed significant increases in the levels of transketolase, Atp5b, creatinekinase B-type, and isocitrate dehydrogenase (Table 4), linking with the TCA cycle and metabolic pathway. Similar results were described in the proteome analysis of Tg2576 and 3xTgAD mouse brains (Martin et al., 2008). Thus, it is implied that Aβ oligomers could enhance just the phosphorylation levels for these proteins. Based on our study in conjunction with previous reports, Aβ oligomers might play a role in energy metabolism in AD.

4.3. Synaptic component

We identified four spots as Dpysl2, also known as collapsin response mediator protein 2 (CRMP-2), in the hippocampus (Inagaki et al., 2001). This protein inhibits axonal outgrowth and path-finding through the transmission and modulation of extracellular signals, and Aβ 40 oligomers also inhibited neurite outgrowth on neuroblastoma SH-SY5Y cells, thereby suggesting that neurite outgrowth inhibited by Aß may be initiated through a mechanism in which Aβ increases CRMP-2 to interfere with tubulin assembly in neuritis (Petratos et al., 2008). The protein level of Dpysl2 was increased in $APP_{E693\Delta}$-transgenic mice, which is consistent with the results of Tg2576 mice (Martin et al., 2008). Based on our findings in conjunction with previous reports, it is suggested that Aβ oligomers promote abnormal neurological changes of AD by increasing Dpysl2.

4.4. Vesicle transport and recycling

Dynamin, a well studied neuron-specific mechanochemical GTPase, pinches off synaptic vesicles, freeing them from the membrane and allowing them to re-enter the synaptic vesicle pool to be refilled for future release (Kelly et al., 2005). Our results in $APP_{E693\Delta}$-transgenic mice without plaque deposition are consistent with previous findings that protein levels of dynamin were increased in Tg2576 mice with plaque deposition (Shin et al., 2004), suggesting that dynamin may be increased irrespective of AD stage.

5. Conclusions

In summary, we identified altered levels of some proteins and phosphoproteins in $APP_{E693\Delta}$-transgenic mouse hippocampus and cortex. As mentioned above, $APP_{E693\Delta}$-transgenic mice exhibit only Aβ oligomers in the brain, which makes them a good model to investigate the pathological effects of Aβ oligomers avoiding the influence of amyloid plaques. Thus, we concluded that the altered levels of proteins and phosphoproteins expression we detected in $APP_{E693\Delta}$-transgenic mice were induced just by Aβ oligomers. Our findings might provide a clue for investigation of the pathogenesis of AD, especially the early stage of AD. Further study will be required to elucidate the precise mechanisms underlying Aβ oligomer-induced proteomic alterations.

Acknowledgements

This work was supported by grants from the Smoking Research Foundation, Kobe Gakuin University for Collaborative Research B, and Kobe Gakuin University Life Science Center. Also supported by the Grants-in-Aid for Scientific Research from the Ministry of Education, Culture, Sports, Science and Technology of Japan (no. 18023033, 21500352, 21390271, 20023027); by the Grants-in-Aid for Comprehensive Research on Dementia from the Ministry of Health, Labour and Welfare, Japan; and in part by the Alzheimer's Association (IIRG-09-132098).

Appendix A. Supplementary data

Supplementary data associated with this article can be found, in the online version, at http://dx.doi.org/10.1016/j.neuint.2012.05.018.

References

Akiyama, H., Barger, S., Barnum, S., Bradt, B., Bauer, J., Cole, G.M., Cooper, N.R., Eikelenboom, P., Emmerling, M., Fiebich, B.L., Finch, C.E., Frautschy, S., Griffin, W.S., Hampel, H., Hull, M., Landreth, G., Lue, L., Mrak, R., Mackenzie, I.R., McGeer, P.L., O'Banion, M.K., Pachter, J., Pasinetti, G., Plata-Salaman, C., Rogers, J., Rydel, R., Shen, Y., Streit, W., Strohmeyer, R., Tooyoma, I., Van Muiswinkel, F.L., Veerhuis, R., Walker, D., Webster, S., Wegrzyniak, B., Wenk, G., Wyss-Coray, T., 2000. Inflammation and Alzheimer's disease. Neurobiol. Aging 21, 383–421.

Birbach, A., 2008. Profilin, a multi-modal regulator of neuronal plasticity. BioEssays 30, 994–1002.

Fulga, T.A., Elson-Schwab, I., Khurana, V., Steinhilb, M.L., Spires, T.L., Hyman, B.T., Feany, M.B., 2007. Abnormal bundling and accumulation of F-actin mediates tau-induced neuronal degeneration in vivo. Nat. Cell Biol. 9, 139–148.

Glenner, G.G., Wong, C.W., 1984. Alzheimer's disease: initial report of the purification and characterization of a novel cerebrovascular amyloid protein. Biochem. Biophys. Res. Commun. 120, 885–890.

Gorg, A., Obermaier, C., Boguth, G., Harder, A., Scheibe, B., Wildgruber, R., Weiss, W., 2000. The current state of two-dimensional electrophoresis with immobilized pH gradients. Electrophoresis 21, 1037–1053.

Hardy, J., Selkoe, D.J., 2002. The amyloid hypothesis of Alzheimer's disease: progress and problems on the road to therapeutics. Science 297, 353–356.

Hoyer, S., 2004. Causes and consequences of disturbances of cerebral glucose metabolism in sporadic Alzheimer disease: therapeutic implications. Adv. Exp. Med. Biol. 541, 135–152.

Inagaki, N., Chihara, K., Arimura, N., Menager, C., Kawano, Y., Matsuo, N., Nishimura, T., Amano, M., Kaibuchi, K., 2001. CRMP-2 induces axons in cultured hippocampal neurons. Nat. Neurosci. 4, 781–782.

Kelly, B.L., Vassar, R., Ferreira, A., 2005. Beta-amyloid-induced dynamin 1 depletion in hippocampal neurons. A potential mechanism for early cognitive decline in Alzheimer disease. J. Biol. Chem. 280, 31746–31753.

Klein, W.L., Krafft, G.A., Finch, C.E., 2001. Targeting small Abeta oligomers: the solution to an Alzheimer's disease conundrum? Trends Neurosci. 24, 219–224.

Kuhn, T.B., Meberg, P.J., Brown, M.D., Bernstein, B.W., Minamide, L.S., Jensen, J.R., Okada, K., Soda, E.A., Bamburg, J.R., 2000. Regulating actin dynamics in neuronal growth cones by ADF/cofilin and rho family GTPases. J. Neurobiol. 44, 126–144.

Lee, V.M., Goedert, M., Trojanowski, J.Q., 2001. Neurodegenerative tauopathies.. Ann. Rev. Neurosci. 24, 1121–1159.

Li, S., Hong, S., Shepardson, N.E., Walsh, D.M., Shankar, G.M., Selkoe, D., 2009. Soluble oligomers of amyloid beta protein facilitate hippocampal long-term depression by disrupting neuronal glutamate uptake. Neuron 62, 788–801.

Martin, B., Brenneman, R., Becker, K.G., Gucek, M., Cole, R.N., Maudsley, S., 2008. ITRAQ analysis of complex proteome alterations in 3xTgAD Alzheimer's mice. Understanding the interface between physiology and disease. PLoS ONE 3, e2750.

Minamide, L.S., Striegl, A.M., Boyle, J.A., Meberg, P.J., Bamburg, J.R., 2000. Neurodegenerative stimuli induce persistent ADF/cofilin-actin rods that disrupt distal neurite function. Nat. Cell Biol. 2, 628–636.

Nunomura, A., Perry, G., Aliev, G., Hirai, K., Takeda, A., Balraj, E.K., Jones, P.K., Ghanbari, H., Wataya, T., Shimohama, S., Chiba, S., Atwood, C.S., Petersen, R.B., Smith, M.A., 2001. Oxidative damage is the earliest event in Alzheimer disease. J. Neuropathol. Exp. Neurol. 60, 759–767.

Otani, M., Taniguchi, T., Sakai, A., Seta, J., Kadoyama, K., Nakamura-Hirota, T., Matsuyama, S., Sano, K., Takano, M., 2011. Phosphoproteome profiling using a fluorescent phosphosensor dye in two-dimensional polyacrylamide gel electrophoresis. Appl. Biochem. Biotechnol. 164, 804–818.

Petratos, S., Li, Q.X., George, A.J., Hou, X., Kerr, M.L., Unabia, S.E., Hatzinisiriou, I., Maksel, D., Aguilar, M.I., Small, D.H., 2008. The beta-amyloid protein of Alzheimer's disease increases neuronal CRMP-2 phosphorylation by a Rho-GTP mechanism.. Brain: J. Neurol. 131, 90–108.

Provost, P., Doucet, J., Stock, A., Gerisch, G., Samuelsson, B., Radmark, O., 2001. Coactosin-like protein, a human F-actin-binding protein: critical role of lysine-75. Biochem. J. 359, 255–263.

Selkoe, D.J., 2002. Alzheimer's disease is a synaptic failure. Science 298, 789–791.

Shin, S.J., Lee, S.E., Boo, J.H., Kim, M., Yoon, Y.D., Kim, S.I., Mook-Jung, I., 2004. Profiling proteins related to amyloid deposited brain of Tg2576 mice. Proteomics 4, 3359–3368.

Sultana, R., Boyd-Kimball, D., Cai, J., Pierce, W.M., Klein, J.B., Merchant, M., Butterfield, D.A., 2007. Proteomics analysis of the Alzheimer's disease hippocampal proteome. J. Alzheimers Dis. 11, 153–164.

Takano, M., Otani, M., Sakai, A., Kadoyama, K., Matsuyama, S., Matsumoto, A., Takenokuchi, M., Sumida, M., Taniguchi, T., 2009. Use of a phosphosensor dye in proteomic analysis of human mutant tau transgenic mice. NeuroReport 20, 1648–1653.

Tomiyama, T., Matsuyama, S., Iso, H., Umeda, T., Takuma, H., Ohnishi, K., Ishibashi, K., Teraoka, R., Sakama, N., Yamashita, T., Nishitsuji, K., Ito, K., Shimada, H., Lambert, M.P., Klein, W.L., Mori, H., 2011. A mouse model of amyloid beta oligomers: their contribution to synaptic alteration, abnormal tau phosphorylation, glial activation, and neuronal loss in vivo. J. Neurosci. 30, 4845–4856.

Tomiyama, T., Nagata, T., Shimada, H., Teraoka, R., Fukushima, A., Kanemitsu, H., Takuma, H., Kuwano, R., Imagawa, M., Ataka, S., Wada, Y., Yoshioka, E., Nishizaki, T., Watanabe, Y., Mori, H., 2008. A new amyloid beta variant favoring oligomerization in Alzheimer's-type dementia. Ann. Neurol. 63, 377–387.

Vanhanen, M., Koivisto, K., Moilanen, L., Helkala, E.L., Hanninen, T., Soininen, H., Kervinen, K., Kesaniemi, Y.A., Laakso, M., Kuusisto, J., 2006. Association of metabolic syndrome with Alzheimer disease: a population-based study. Neurology 67, 843–847.

Whiteman, I.T., Gervasio, O.L., Cullen, K.M., Guillemin, G.J., Jeong, E.V., Witting, P.K., Antao, S.T., Minamide, L.S., Bamburg, J.R., Goldsbury, C., 2009. Activated actin-depolymerizing factor/cofilin sequesters phosphorylated microtubule-associated protein during the assembly of Alzheimer-like neuritic cytoskeletal striations. J. Neurosci. 29, 12994–13005.

Yokoyama, Y., Kuramitsu, Y., Takashima, M., Iizuka, N., Toda, T., Terai, S., Sakaida, I., Oka, M., Nakamura, K., Okita, K., 2004. Proteomic profiling of proteins decreased in hepatocellular carcinoma from patients infected with hepatitis C virus. Proteomics 4, 2111–2116.

Neuroscience Letters 534 (2013) 85–89

Contents lists available at SciVerse ScienceDirect

Neuroscience Letters

journal homepage: www.elsevier.com/locate/neulet

Proteomic analysis of the hippocampus in Alzheimer's disease model mice by using two-dimensional fluorescence difference in gel electrophoresis

Masaoki Takano[a], Takuya Yamashita[b,c], Kazuya Nagano[c], Mieko Otani[a], Kouji Maekura[a], Haruhiko Kamada[c], Shin-ichi Tsunoda[c], Yasuo Tsutsumi[b,c], Takami Tomiyama[e,f], Hiroshi Mori[e,f], Kenji Matsuura[d], Shogo Matsuyama[d,*]

[a] Laboratory of Molecular Cellular Biology, School of Pharmaceutical Sciences, Kobe Gakuin University, 1-1-3 Minatojima, Chuo-ku, Kobe 650-8586, Japan
[b] Laboratory of Toxicology and Safety Science, Graduate School of Pharmaceutical Sciences, Osaka University, 1-6 Yamadaoka, Suita, Osaka 565-0871, Japan
[c] Laboratory of Biopharmaceutical Research, National Institute of Biomedical Innovation, 7-6-8 Saito-Asagi, Ibaraki, Osaka 567-0085, Japan
[d] Faculty of Pharmaceutical Sciences, Himeji Dokkyo University, 7-2-1 Kamiohno, Himeji 670-8524, Japan
[e] Department of Neuroscience, Osaka City University Graduate School of Medicine, Osaka 545-8585, Japan
[f] Core Research for Evolutional Science and Technology, Japan Science and Technology Agency, Japan

HIGHLIGHTS

- We perform the proteome for $APP_{E693\Delta}$-transgenic mice. Methods are two-dimensional fluorescence difference in gel electrophoresis and mass spectrometry techniques. The expression of 14 proteins are changed in the brain. Aβ oligomers contribute to the expression of proteins.

ARTICLE INFO

Article history:
Received 4 August 2012
Received in revised form 13 October 2012
Accepted 6 November 2012

Keywords:
Proteome
Amyloid β oligomers
Alzheimer's disease
Hippocampus
2D-DIGE

ABSTRACT

We previously identified the E693Δ mutation in amyloid precursor protein (APP) in patients with Alzheimer's disease (AD) and then generated APP-transgenic mice expressing this mutation. As these mice possessed abundant Aβ oligomers from 8 months of age but no amyloid plaques even at 24 months of age, they are a good model to study pathological effects of amyloid β (Aβ) oligomers. The two-dimensional fluorescence difference in gel electrophoresis (2D-DIGE) technology, using a mixed-sample internal standard, is now recognized as an accurate method to determine and quantify proteins. In this study, we examined the proteins for which levels were altered in the hippocampus of 12-month-old $APP_{E693\Delta}$-transgenic mice using 2D-DIGE and liquid chromatography–tandem mass spectrometry (LC–MS/MS). Fourteen proteins were significantly changed in the hippocampus of $APP_{E693\Delta}$-transgenic mice. Actin cytoplasmic 1 (β-actin), heat shock cognate 71 kDa, γ-enolase, ATP synthase subunit β, tubulin β-2A chain, clathrin light chain B (clathrin) and dynamin-1 were increased. Heat shock-related 70 kDa protein 2, neurofilament light polypeptide (NFL), stress-induced-phosphoprotein 2, 60 kDa heat shock protein (HSP60), α-internexin, protein kinase C and casein kinase substrate in neurons protein 1 (Pacsin 1), α-enolase and β-actin were decreased. Western blotting also validated the changed levels of HSP60, NFL, clathrin and Pacsin 1 in $APP_{E693\Delta}$-transgenic mice. The identified proteins could be classified as cytoskeleton, chaperons, neurotransmission, energy supply and signal transduction. Thus, proteomics by 2D-DIGE and LC–MS/MS has provided knowledge of the levels of proteins in the early stages of AD brain.

1. Introduction

AD is neuropathologically characterized by abnormal accumulation of extracellular amyloid plaques and intracellular neurofibrillary tangles throughout cortical and limbic regions. Although the current amyloid cascade hypothesis [6] and tau hypothesis [15] provide frameworks for studying AD pathogenesis. Recently, diverse lines of evidence suggest that Aβ peptides play more important roles in AD pathogenesis [13,16,20]. Especially, soluble oligomers of Aβ could be a cause of synaptic and cognitive dysfunction in the early stages of AD. To address the relationship between Aβ oligomers and pathological features of AD, we generated APP transgenic mice expressing the E693Δ mutation, which enhanced Aβ oligomerization without fibrillization [25]. It might provide a clue for elucidating AD pathology caused by Aβ oligomers to analyze the $APP_{E693\Delta}$-transgenic mice.

* Corresponding author. Tel.: +81 79 223 6849; fax: +81 79 223 6857.
E-mail address: shogo@himeji-du.ac.jp (S. Matsuyama).

0304-3940/$ – see front matter © 2012 Elsevier Ireland Ltd. All rights reserved.
http://dx.doi.org/10.1016/j.neulet.2012.11.010

One of the most utilized approaches in proteomics to quantify and identify proteins is two dimensional gel electrophoresis (2DE) and mass spectrometry (MS) [5]. Proteomic approaches were most widely based on methods using differential expression on 2D-PAGE gels, or more recently 2D chromatography, followed by mass spectrometry protein identification. Compared to these conventional analyses, 2D-DIGE has higher reproducibility and sensitivity because of its internal standard design which minimizes gel-to-gel variation, improves spot matching, reduces number of gels needed, and permits quantitative analysis of small sample amounts.

In this study, we studied the altered expression of proteins in the hippocampus of $APP_{E693\Delta}$-transgenic mice using 2D-DIGE and LC–MS/MS approach. This approach revealed that the levels of at least 14 proteins were altered in the hippocampus of 12-month-old $APP_{E693\Delta}$-transgenic mice. These findings suggest that Aβ oligomers might cause synaptic and cognitive dysfunction by affecting the expression of these proteins in the hippocampus.

2. Experimental procedures

2.1. Materials

Sodium dodecyl sulfate, urea, thiourea, CHAPS, dithiothreitol, iodoacetamide, bromophenol blue, and RNase A and DNase I for SDS-PAGE or 2DE were all obtained from Wako Pure Chemical Industries (Osaka, Japan). Source information for all other assay reagents and materials are incorporated into their respective assay methods described below.

2.2. Animal subjects

Transgenic mice expressing human APP_{695} with the APP E693Δ mutation under the mouse prion promoter were used [25]. Heterozygous human $APP_{E693\Delta}$-transgenic mice and age-matched non-transgenic littermates were sacrificed at 12 months of age, and their hippocampi were isolated on an ice-cold plate. Animal care and handling were performed strictly in accordance with the Guidelines for Animal Experimentation at Kobe Gakuin University and Himeji Dokkyo University. Every effort was made to minimize the number of animals used and their suffering.

2.3. Protein labeling with CyDyes

Equal amounts of total protein from 4 hippocampi of $APP_{E693\Delta}$-transgenic mice or age-matched non-transgenic littermates were separately pooled. Protein samples were labeled with CyDyes (GE Healthcare, Piscataway, NJ), as per manufacturer's instructions. In brief, 50 μg of total protein from each sample was mixed in a tube and labeled with Cy2 minimal dye, and 50 μg protein taken from the mix was used as an internal standard on each gel for the three subsequent 2DE and image analysis. In parallel, 50 μg protein from each sample was labeled with either Cy3 or Cy5, and the dyes scrambled within each group to avoid possible dye bias. As a result, one replicate was Cy3 labeled proteins and another replicate was Cy5 labeled proteins. Two replicates (Cy3 and Cy5 labeled samples) were mixed, divided and applied each three independent gels. The sample volumes were adjusted to 18 μL with labeling buffer (7M urea, 2 M thiourea, 4% CHAPS, 30 mM Tris), followed by addition of 1 μL dye (working solution) to each individual sample. The samples were left on ice for 30 min in the dark, followed by adding 1 μL of 10 mmol/L lysine to stop the reaction.

2.4. 2D electrophoresis and image analysis

One sample from each of the CyDye groups was mixed together and adjusted to final concentrations of 1% DTT, 1% IPG buffer at a total volume of 350 μL with lysis buffer (7 M urea, 2 M thiourea, 4% CHAPS) and was used to 24 cm pH 4–7 IPG strips (non-linear; GE Healthcare, Piscataway, NJ) overnight. First dimension isoelectric focusing (IEF) was carried out with IPGphor II (GE Healthcare, Piscataway, NJ). Second dimension SDS-PAGE was performed by mounting the IPG strips onto 20 × 26 cm 12.5% DIGE gels (GE Healthcare, Piscataway, NJ) using Ettan DALT six Large Electrophoresis System (GE Healthcare, Piscataway, NJ) and running the gels at 16 mA/gel for the initial hour and 25 mA/gel at 25 °C constantly until bromophenol blue reached the bottom of the gel. The lysates were labeled at the ratio of 50 μg proteins: 400 pmol Cy3 or Cy5 protein-labeling dye (GE HealthcareBiosciences) in dimethylformamide according to the manufacturer's protocol.

In summary, three analytical gels were completed in total, running 25 μg of pooled reference sample labeled with Cy2, along with two samples (25 μg each), one labeled with Cy3 and the other labeled with Cy5. Gels selected for picking were stained with Deep purple (GE Healthcare, Piscataway, NJ). Approximately 1100 spots were matched across all three analytical gels. The analytical gel was picked using an automated robotic system, Ettan Spot picker (GE Healthcare, Piscataway, NJ). The pick list was created based on the Deep purple image. 2 mm gel plugs were picked, washed, reduced and alkylated, and then digested with trypsin, and the resulting peptides were extracted. Gel trypsinization was performed as previously described [24].

2.5. LC/MS/MS identification

Trypsinized peptides were analyzed by nano LC/MS/MS on a ThermoFisher LTQ Orbitrap XL. In brief, 30 mL of hydrolysate was loaded onto a 5 mm 675 mm ID C12 (Jupiter Proteo, Phenomenex) vented column at a flow-rate of 10 mL/min. Gradient elution was conducted on a 15 cm by 75 mm ID C12 column at 300 nL/min. A 30 min gradient was employed. The mass spectrometer was operated in a data-dependent mode, and the six most abundant ions were selected for MS/MS. Mass spectrometry results were searched using Mascot (www.matrixscience.com). Samples were processed in the Scaffold algorithm using DAT files generated by Mascot. Parameters for LTQ Orbitrap XL data require a minimum of two peptide matches per protein with minimum probabilities of 90% at the protein level.

2.6. Western blotting

Approximately 25 μg of protein from mouse hippocampus was applied to a 12.5% acrylamide gel and SDS-polyacrylamide gel electrophoresis was performed at 17.5 mA/gel for 2 h in second dimension. The gels were transferred onto PVDF membranes (Pall Corporation, Pensacola, FL, USA), in a trans-blot electrophoresis transfer cell (Nihon Eido, Tokyo, Japan). Western blotting was performed by using monoclonal antibodies against β-actin (diluted 1:1000, Cell Signaling, USA) and clathrin (diluted 1:250, Abcam, USA), polyclonal antibodies HSP60, NFL, voltage-dependent anion-selective channel protein 1 (VDAC) (diluted 1:1000, Cell Signaling, USA) and Pacsin 1 (diluted 1:500, Millipore, USA). Peroxidase-conjugated antibody (diluted 1:5000, Abcam, USA) was used as secondary antibody. The reaction was detected by chemiluminescence with ECL reagents (Pierce Biotechnology, USA). A semi quantitative analysis based on optical density was performed by ImageJ software (available at http://www.rsbweb.nih.gov/ij).

3. Results and discussion

The 2D-DIGE gels of the hippocampi from wild type and $APP_{E693\Delta}$-transgenic mice pools were shown as Fig. 1. Two replicates of each pooled sample were run, labeling one replicate with

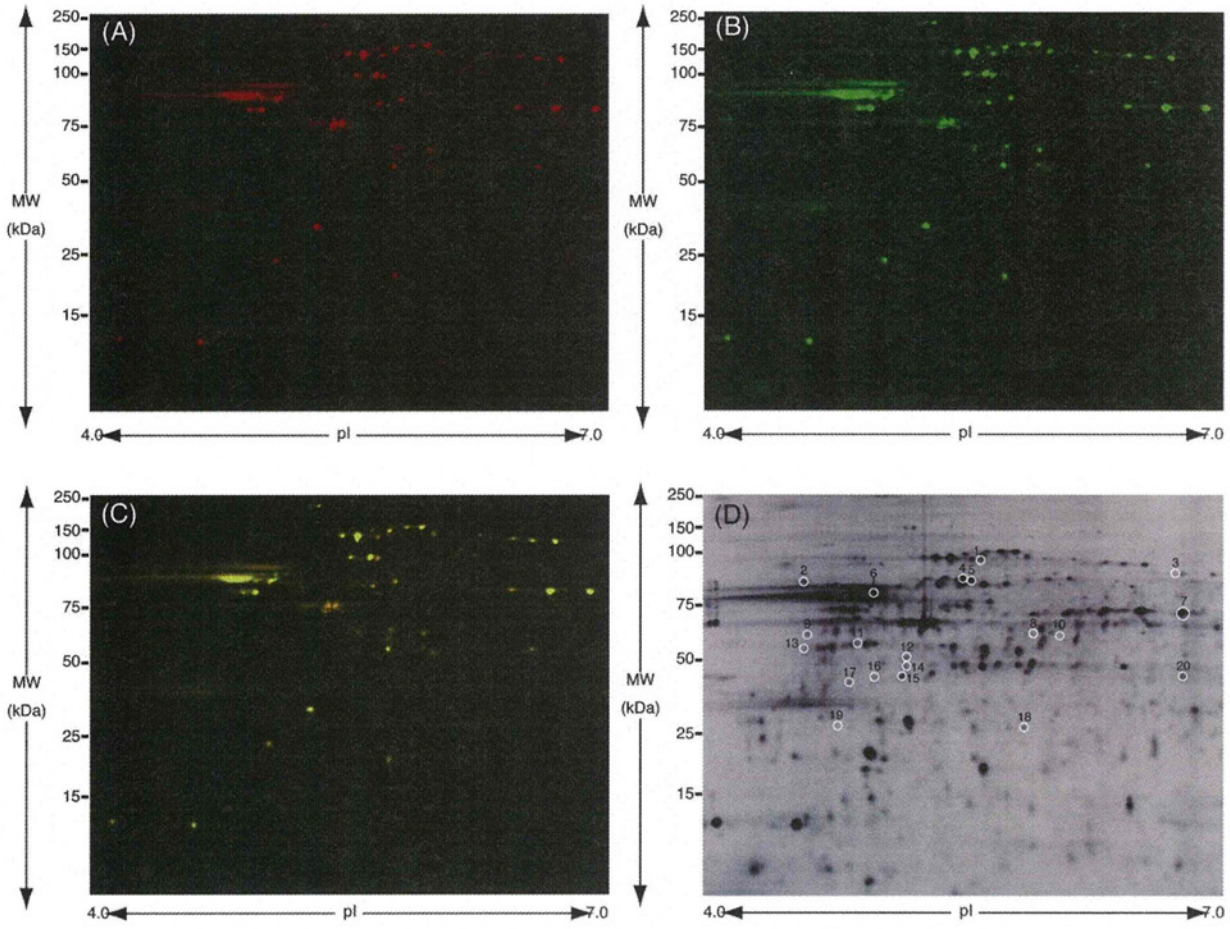

Fig. 1. 2D-DIGE gel image of fluorescence-labeled hippocampal proteins of non-transgenic and $APP_{E693\Delta}$-transgenic mice. (A) Analysis of the proteome of non-transgenic mice hippocampi with Cy3 Dye. (B) $APP_{E693\Delta}$-transgenic mice hippocampi with Cy5 Dye. (C) Merged. (D) Fourteen protein spots identified from non-transgenic and $APP_{E693\Delta}$-transgenic mice hippocampi by LC/MS/MS. Black numbers with white circles indicate proteins that are listed in Table 1.

Cy3 (Fig. 1A) and one replicate with Cy5 (Fig. 1B), resulting in three analytical gels. The 2D-DIGE comparative analysis of the wild type and $APP_{E693\Delta}$-transgenic mice revealed significant 74 spots (Fig. 1C). These spots were investigated by LC–MS/MS (Fig. 1D). Finally, fourteen proteins were identified as shown in Table 1. These proteins are classified into several groups that are involved in cytoskeletal, chaperone, energy metabolic, vesicle transport and signaling proteins (Table 2).

Spot nos. 1, 3 and 4 were identified as heat shock-related 70 kDa protein 2, stress-induced-phosphoprotein 1 and HSP60, respectively. The stress-induced-phosphoprotein 1 is the co-chaperone and thought of the function in regulation of interaction with Hsp70 and Hsp90 [10]. HSP60 is the chaperonin which is implicated in mitochondrial protein import and macromolecular assembly and may facilitate the correct folding of imported proteins [9]. The amounts of heat shock-related 70 kDa protein 2, stress-induced-phosphoprotein 1, and HSP60 were significantly decreased. On the contrary, spot no. 9 which was identified as heat shock cognate 71 kDa protein was significantly increased. This protein is also the chaperone and acts as a repressor of transcriptional activation [8]. Thus, Aβ oligomers might contribute to changing the expression of the chaperons.

Spot nos. 8, 10–12 and 16 were identified as actin, and spot nos. 15 and 17 were identified as tubulin β-2A chain. Actin is one of the major cytoskeletal proteins in neurons, and the dynamics of its assembly are involved in many aspects of cell motility, vesicle transport, and membrane turnover [14]. Actin itself is known to link with Aβ, which enhances the neurotoxicity induced by tau-mediated actin filament formation [4]. The four spots of actin but not no. 12 and those of tubulin were significantly increased. Thus, Aβ oligomers might lead to increasing the amounts of actin and tubulin.

Spot nos. 5 and 2 were identified as α-internexin and NFL, respectively, which are known as neuronal intermediate proteins [2,18]. The amounts of α-internexin and NFL were significantly decreased. Thus, the decreased amounts of NFL and internexin might raise neural dysfunction in the hippocampus of AD.

Spot nos. 7 and 13 were identified as α-enolase. Spot nos. 14 and 19 were identified as γ-enolase and ATP synthase subunit β, respectively. Enolase is a multifunctional protein as glycolytic enzyme, belonging to a novel class of surface proteins [11]. ATP synthase is a key role enzyme that provides energy for the cell to use through the synthesis of ATP [1]. The amount of α-enolase was significantly decreased, but the amounts of γ-enolase and ATP synthase subunit β were significantly increased. Interestingly, the levels of α-enolase and ATP synthase subunit α mitochondrial proteins significantly increased in the hippocampus of J20 Tg mice with amyloid deposition [19]. The amyloid deposit enhanced the expression of energy metabolic proteins [22]. Combined with our findings, both Aβ oligomers and amyloid deposition might play an important role in the change of energy metabolic proteins as α-enolase, γ-enolase and ATP synthase subunit β.

Spot no. 20 was identified as dynamin. Dynamin, a well studied neuron-specific mechanochemical GTPase, pinches off synaptic vesicles, freeing them from the membrane and allowing them to re-enter the synaptic vesicle pool to be refilled for future release

Table 1
Identified proteins from differentially expressed in the hippocampus of$APP_{E693\Delta}$-transgenic mice when compared to non-transgenic littermates.

Spot no.	Protein ID	Fold (APP/WT)	*t*-Test	Accession	Coverage	#Peptides	Predicted MW (kDa)	Calc. pI	Score
1	Heat shock-related 70 kDa protein 2	−1.32	0.040	P14659	26.22	23	69.6	5.67	625.70
2	Neurofilament light polypeptide	−1.48	0.002	P08551	39.96	43	61.5	4.64	1004.84
3	Stress-induced-phosphoprotein 1	−1.44	0.002	Q60864	16.21	9	62.5	6.80	157.49
4	60 kDa heat shock protein	−1.36	0.013	P63038	52.71	71	60.9	6.18	1916.39
5	Alpha-internexin	−1.34	0.023	P46660	42.66	39	55.7	5.27	1119.47
6	Protein kinase C and cascin kinase substrate in neurons protein 1	−1.48	0.023	Q61644	28.34	15	50.5	5.24	356.92
7	Alpha-enolase	−1.32	0.000	P17182	34.33	24	47.1	6.80	474.21
8	Actin, cytoplasmic 1	1.51	0.003	P60709	25.87	14	41.7	5.48	231.79
9	Heat shock cognate 71 kDa protein	1.35	0.015	P63017	12.54	16	70.8	5.52	319.85
10	Actin, cytoplasmic	1.34	0.004	P60709	24.27	13	41.7	5.48	279.37
11	Actin, cytoplasmic 1	1.38	0.022	P60709	15.47	7	41.7	5.48	243.14
12	Actin, cytoplasmic 1	−1.56	0.013	P60709	22.67	12	41.7	5.48	131.57
13	Gamma-enolase	1.33	0.005	P17183	20.05	13	47.3	5.11	237.25
14	ATP synthase subunit beta	1.40	0.047	P56480	23.60	18	56.3	5.34	356.19
15	Tubulin beta-2A chain	1.31	0.021	Q13885	14.83	13	49.9	4.89	313.07
16	Actin, cytoplasmic 1	1.47	0.002	P60709	6.93	3	41.7	5.48	97.01
17	Tubulin beta-2S chain	1.44	0.009	Q13885	11.46	5	49.9	4.89	118.50
18	Clathrin light chain B	1.68	0.005	P09497	8.30	3	25.2	4.64	95.06
19	ATP synthase subunit beta	1.46	0.013	P06576	16.64	16	56.5	5.40	283.06
20	Dynamin-1	1.40	0.006	Q05193	9.61	13	97.3	7.17	242.16

Mass spectrometry protein identification of 2D-DIGE spots of interest and statistical analysis using *t*-test between wild type mice and $APP_{E693\Delta}$-transgenic mice gels ($P < 0.05$). The proteins of mouse hippocampus were separated by 2DE and identified by LC MS/MS, following in-gel digestion with trypsin. The spots representing identified proteins are indicated in Fig. 1D and are designated with their ID accession numbers of Swiss Prot database. Score relates to the probability assignment. Score and sequence coverage were calculated by MASCOT search engine (http://www.matrixscience.com).

Table 2
Functions regulated by proteins that showed an altered expression in $APPE_{693\Delta}$-transgenic mouse hippocampus.

Function	Identified protein	Up/down
Cytoskeletal and their interacting proteins	Neurofilament light polypeptide	Down
	Alpha-internexin	Down
	Actin, cytoplasmic 1	Up/down
	Tubulin β-2A Chain	Up
Chaperone and their interacting proteins	Stress-induced-phosphoprotein 1	Down
	60 kDa heat shock protein	Down
	Heat shock cognate 71 kDa protein	Down
Energy metabolic proteins	Alpha-enolase	Down
	Gamma-enolase	Up
	ATP synthase subunit beta	Up
Vesicle transport and recycling	Dynamin-1	Up
	Clathrin light chain B	Up
Signaling proteins	Protein kinase C and casein kinase substrate in neurons protein 1	Down

The analysis of proteins function was done by using MOTIF (http://www.genome.jp/tools/motif/).

[12]. The amount of dynamin was significantly increased. Our findings in $APP_{E693\Delta}$-transgenic mice without plaque deposition are consistent with previous findings that protein levels of dynamin were increased in Tg2576 mice with plaque deposition [21], suggesting that the release of neurotransmitter is affected by dynamin increased irrespective of AD stage. Also, spot no. 6 was identified as Pacsin 1. The Pacsin 1 is colocalized, oligomerized and bound with dynamin, and both proteins participate in synaptic vesicle endocytosis [17]. The amount of Pacsin 1 was significantly increased. Taken together, Pacsin 1 and dynamin enhanced by Aβ oligomers

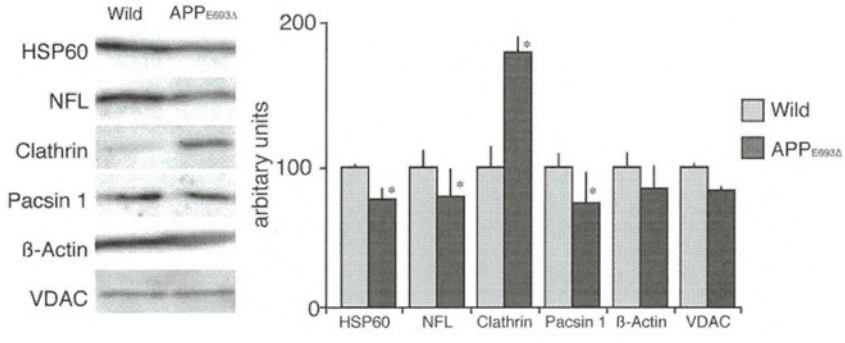

Fig. 2. Differentially expressed proteins validated by Western blotting for the hippocampus of non-transgenic and $APP_{E693\Delta}$-transgenic mice. (A) The levels of HSP60, NFL, clathrin, Pacsin 1, β-actin and VDAC in individual samples of each group were detected. (B) Graphical representation of the semi quantitative analysis (mean ± SEM of O.D. of bands). Data are presented as mean ± SEM ($n = 4$) *t*-test; *$P < 0.05$ vs. $APP_{E693\Delta}$-transgenic mice.

might change the function of synaptic vesicle in the hippocampus of AD.

Spot no. 18 was identified as clathrin, which is known as the major protein of the polyhedral coat of coated pits and vesicles [7]. The amount of spot no. 18 was significantly decreased. APP was associated clusters of clathrin-coated vesicles and endosomes [3]. Thus, Aβ oligomers might inhibit the vesicle formation by clathrin.

In addition, we performed a validation experiment for HSP60, NFL, clathrin, Pacsin 1 and β-actin as the altered proteins, and VDAC as the unchanged protein (as control) [23]. The increased levels of clathrin, the decreased levels of HSP60, NFL, and Pacsin 1 and the unchanged level of β-actin and VDAC in $APP_{E693\Delta}$-transgenic mice hippocampus were validated by Western blotting (Fig. 2).

In summary, we identified the altered levels of 14 proteins in $APP_{E693\Delta}$-transgenic mice hippocampus using 2D-DIGE and LC–MS/MS approach. This approach elucidated the pathological effects of Aβ oligomers on hippocampus. Our findings might provide a clue for investigation of the hippocampus of AD early stage.

Acknowledgements

This work was supported by grants from Kobe Gakuin University for Collaborative Research C and the Smoking Research Foundation. The authors thank Dr. Tadanori Mayumi for his encouragement during the early days of the study.

References

[1] U. Andersson, H. Antonicka, J. Houstek, B. Cannon, A novel principle for conferring selectivity to poly(A)-binding proteins: interdependence of two ATP synthase beta-subunit mRNA-binding proteins, Biochemical Journal 346 (Pt 1) (2000) 33–39.
[2] C.L. Chien, R.K. Liem, Characterization of the mouse gene encoding the neuronal intermediate filament protein alpha-internexin, Gene 149 (1994) 289–292.
[3] A. Ferreira, A. Caceres, K.S. Kosik, Intraneuronal compartments of the amyloid precursor protein, Journal of Neuroscience 13 (1993) 3112–3123.
[4] T.A. Fulga, I. Elson-Schwab, V. Khurana, M.L. Steinhilb, T.L. Spires, B.T. Hyman, M.B. Feany, Abnormal bundling and accumulation of F-actin mediates tau-induced neuronal degeneration in vivo, Nature Cell Biology 9 (2007) 139–148.
[5] A. Gorg, C. Obermaier, G. Boguth, A. Harder, B. Scheibe, R. Wildgruber, W. Weiss, The current state of two-dimensional electrophoresis with immobilized pH gradients, Electrophoresis 21 (2000) 1037–1053.
[6] J. Hardy, D.J. Selkoe, The amyloid hypothesis of Alzheimer's disease: progress and problems on the road to therapeutics, Science 297 (2002) 353–356.
[7] J. Hirst, M.S. Robinson, Clathrin and adaptors, Biochimica et Biophysica Acta 1404 (1998) 173–193.
[8] C.R. Hunt, A.J. Parsian, P.C. Goswami, C.A. Kozak, Characterization and expression of the mouse Hsc70 gene, Biochimica et Biophysica Acta 1444 (1999) 315–325.
[9] S. Ikawa, R.A. Weinberg, An interaction between p21ras and heat shock protein hsp60, a chaperonin, Proceedings of the National Academy of Sciences 89 (1992) 2012–2016.
[10] J.L. Johnson, A. Halas, G. Flom, Nucleotide-dependent interaction of Saccharomyces cerevisiae Hsp90 with the cochaperone proteins Sti1, Cpr6, and Sba1, Molecular and Cellular Biology 27 (2007) 768–776.
[11] M. Kaghad, X. Dumont, P. Chalon, J.M. Lelias, N. Lamande, M. Lucas, M. Lazar, D. Caput, Nucleotide sequences of cDNAs alpha and gamma enolase mRNAs from mouse brain, Nucleic Acids Research 18 (1990) 3638.
[12] B.L. Kelly, R. Vassar, A. Ferreira, Beta-amyloid-induced dynamin 1 depletion in hippocampal neurons. A potential mechanism for early cognitive decline in Alzheimer disease, Journal of Biological Chemistry 280 (2005) 31746–31753.
[13] W.L. Klein, G.A. Krafft, C.E. Finch, Targeting small Abeta oligomers: the solution to an Alzheimer's disease conundrum? Trends in Neurosciences 24 (2001) 219–224.
[14] T.B. Kuhn, P.J. Meberg, M.D. Brown, B.W. Bernstein, L.S. Minamide, J.R. Jensen, K. Okada, E.A. Soda, J.R. Bamburg, Regulating actin dynamics in neuronal growth cones by ADF/cofilin and rho family GTPases, Journal of Neurobiology 44 (2000) 126–144.
[15] V.M. Lee, M. Goedert, J.Q. Trojanowski, Neurodegenerative tauopathies, Annual Review of Neuroscience 24 (2001) 1121–1159.
[16] S. Li, S. Hong, N.E. Shepardson, D.M. Walsh, G.M. Shankar, D. Selkoe, Soluble oligomers of amyloid Beta protein facilitate hippocampal long-term depression by disrupting neuronal glutamate uptake, Neuron 62 (2009) 788–801.
[17] J. Modregger, B. Ritter, B. Witter, M. Paulsson, M. Plomann, All three PACSIN isoforms bind to endocytic proteins and inhibit endocytosis, Journal of Cell Science 113 (Pt 24) (2000) 4511–4521.
[18] R.A. Nixon, R.K. Sihag, Neurofilament phosphorylation: a new look at regulation and function, Trends in Neurosciences 14 (1991) 501–506.
[19] R.A. Robinson, M.B. Lange, R. Sultana, V. Galvan, J. Fombonne, O. Gorostiza, J. Zhang, G. Warrier, J. Cai, W.M. Pierce, D.E. Bredesen, D.A. Butterfield, Differential expression and redox proteomics analyses of an Alzheimer disease transgenic mouse model: effects of the amyloid-beta peptide of amyloid precursor protein, Neuroscience 177 (2011) 207–222.
[20] D.J. Selkoe, Alzheimer's disease is a synaptic failure, Science 298 (2002) 789–791.
[21] S.J. Shin, S.E. Lee, J.H. Boo, M. Kim, Y.D. Yoon, S.I. Kim, I. Mook-Jung, Profiling proteins related to amyloid deposited brain of Tg2576 mice, Proteomics 4 (2004) 3359–3368.
[22] R. Sultana, D. Boyd-Kimball, J. Cai, W.M. Pierce, J.B. Klein, M. Merchant, D.A. Butterfield, Proteomics analysis of the Alzheimer's disease hippocampal proteome, Journal of Alzheimer's Disease 11 (2007) 153–164.
[23] M. Takano, K. Maekura, M. Otani, K. Sano, T. Nakamura-Hirota, S. Tokuyama, K.S. Min, T. Tomiyama, H. Mori, S. Matsuyama, Proteomic analysis of the brain tissues from a transgenic mouse model of amyloid beta oligomers, Neurochemistry International 61 (2012) 347–355.
[24] M. Takano, M. Otani, A. Sakai, K. Kadoyama, S. Matsuyama, A. Matsumoto, M. Takenokuchi, M. Sumida, T. Taniguchi, Use of a phosphosensor dye in proteomic analysis of human mutant tau transgenic mice, Neuroreport 20 (2009) 1648–1653.
[25] T. Tomiyama, S. Matsuyama, H. Iso, T. Umeda, H. Takuma, K. Ohnishi, K. Ishibashi, R. Teraoka, N. Sakama, T. Yamashita, K. Nishitsuji, K. Ito, H. Shimada, M.P. Lambert, W.L. Klein, H. Mori, A mouse model of amyloid beta oligomers: their contribution to synaptic alteration, abnormal tau phosphorylation, glial activation, and neuronal loss in vivo, Journal of Neuroscience 30 (2010) 4845–4856.